

# Perturbation Spectra in the Warm Inflationary Scenario

A.N. Taylor\* & A. Berera†

\**Institute for Astronomy, Royal Observatory, Blackford Hill, Edinburgh, EH9 3HJ, U.K.*

†*Department of Physics & Astronomy, University of Edinburgh, Edinburgh, EH9 3JZ, U.K.*

\**ant@roe.ac.uk*, †*ab@ph.ed.ac.uk*

We investigate the phenomenology of warm inflation and present generic results about the evolution of the inflaton and radiation fields. The general conditions required for warm inflation to take place are derived and discussed. A comprehensive approach is presented for the generation of thermally induced adiabatic and isocurvature perturbations and the amplitude of their spectra calculated. In addition we derive the ratio of tensor-to-scalar perturbations and find the spectral indices for adiabatic, isocurvature and tensor perturbations formed in the warm inflationary era. These results are presented in a simplified and compact approach that is generally applicable. Our results are illustrated by inflation models with polynomial and exponential potentials. We compare our analytic results against numerical models and find excellent agreement. Finally, presently available data is used to put constraints on warm inflation and we discuss how near-future observations may distinguish the warm inflationary scenario from standard supercooled inflation. The main observable difference is the different scalar-to-tensor ratio, and that the consistency relation between this and the slope of tensor perturbations does not hold for warm inflation.

PACS number(s): 98.80.Cq, 98.80.-k, 98.80.Es

## I. INTRODUCTION

One of the central paradigms in cosmology is the idea of inflation, and its elegant solution to the problems of standard cosmology. In addition inflation provides an explanation for the origin of structure from quantum fluctuations frozen in by crossing the Hubble radius during the rapid expansion. However in the standard inflationary scenario (see e.g. ref [1–5]) the rapid expansion phase and subsequent reheating of the universe back to a radiation dominated model are treated as two separate periods. The motivation for this was both simplicity and the belief that interactions with the field driving inflation would be minimal [6]. The switching on of field interaction dynamics at the end of inflation results in violent re- and pre-heating effects such as a resonant amplification [7] which can lead to generic amplification of perturbations [8–11].

From the point of view of particle physics, interactions are inevitable, and they lead one to consider the effects on inflation of a phenomenological “friction” term describing the decay of the inflaton field into other fields during inflation [12,13]. One result of this is that density perturbations are no longer generated via quantum fluctuations, but are dominated by the larger thermal fluctuations [12,14].

In this paper we consider the warm inflationary scenario [13,15] from the phenomenological point of view. Several types of phenomenological warm inflation models exist in the literature [16–20]. Warm inflation dynamics also has been studied in quantum field theory [21] and some of the phenomenological models can be derived from first principles [14,22–24]. Our purpose here is to determine generic observational features of the warm inflation scenario, without referring to specific models.

The paper is organised as follows. In Section II results are derive for evolution of the inflationary and radiation fields during the slow-roll phase of warm inflation. Assuming the dissipation rate dominates over the expansion rate, a relationship is found between the radiation energy density and the energy density of the inflationary field. The spectrum of adiabatic perturbations is calculated in Section IIIA and its spectral index in Section IIIB. Isocurvature perturbations are also generated during warm inflation and we present a new derivation of them in Section IIIC and of their spectral index in Section IIID. Tensor perturbations are discussed in Section IIIE. We compare our results with standard inflation in Section IIIF. The conditions for ending warm inflation are discussed in Section IV. Our results are illustrated by the specific cases of inflation with polynomial and power-law potentials in Section V. Our analytic expressions are tested against exact numerical models in Section VI, where we find good agreement between the two. In Section VII we discuss observational constraints on warm inflation and how it may be distinguished from the standard inflation scenario by future CMB experiments. Finally, our conclusions are presented in Section VIII. Two appendices are included in the paper. The first deals with a derivation of the thermal fluctuation of the inflationary field, while the second presents new results for generic polynomial and exponential potentials. Throughout this paper, the conventions of [25] are followed.

## II. EVOLUTION OF THE INFLATIONARY AND RADIATION FIELDS

The evolution of the inflaton field,  $\phi$ , is given by

$$\ddot{\phi} + (3H + \Gamma)\dot{\phi} + V' = 0, \quad (1)$$

where  $H \equiv \dot{a}/a$  is the Hubble parameter,  $a$  is the cosmological expansion factor, and  $\Gamma$  is the dissipation coefficient.  $V(\phi)$  is the potential of the inflationary field. We assume a spatially flat universe. A dot denotes differentiation with time and a prime indicates  $d/d\phi$ . The energy-density of the radiation field,  $\rho_\gamma$ , obeys the transfer equation

$$\dot{\rho}_\gamma + 4H\rho_\gamma = \Gamma\dot{\phi}^2, \quad (2)$$

The equations are completed by the Friedmann equation for the evolution of the universe;

$$H^2 = \frac{8\pi}{3m_p^2}(V + \rho_\gamma), \quad (3)$$

where  $m_p$  is the Planck mass. During an inflationary era the potential field dominates both the kinetic energy of the inflationary field and the energy density of the radiation, so the Friedmann equation can be reduced to

$$H^2 = \frac{8\pi}{3m_p^2}V. \quad (4)$$

We assume the slow-roll condition,  $\dot{\phi}^2 \ll V(\phi)$ , throughout the warm inflationary era, yielding

$$\dot{\phi} = -\frac{V'}{3H(1+r)}, \quad (5)$$

where the ratio of the production rate of radiation to the expansion rate,  $r$ , is defined as

$$r \equiv \frac{\Gamma}{3H}, \quad (6)$$

and parameterises the importance of dissipation in the warm inflationary model.

For the dissipation-dominated regime of warm inflation, the dissipation rate,  $\Gamma$ , is much greater than the expansion rate;  $r \gg 1$ . The evolution of the inflaton field during this phase is governed by

$$\dot{\phi} = -\frac{V'}{3rH}. \quad (7)$$

Hence the slow-roll condition can be met even for relatively steep potentials, due to the damping effect of dissipation on the evolution of  $\phi$ .

If we also assume that during warm inflation radiation production is quasi-stable ( $\dot{\rho}_\gamma \ll \Gamma\dot{\phi}^2$ ), equations (2) and (7) give

$$\rho_\gamma \equiv \alpha T^4 = 3r \left( \frac{1}{2}\dot{\phi} \right)^2, \quad (8)$$

where  $\alpha \equiv g_*\pi^2/30$  is the Stefan-Boltzmann constant and  $g_*$  is the number of degrees of freedom for the radiation

field. In the standard cosmology  $g_* \approx 100$ . Equation (8) shows that the energy density in the radiation field is controlled by the kinetic energy of the inflationary field as well as the dimensionless dissipation rate. As the kinetic energy of  $\phi$  is small during the slow-roll regime we require  $r$  to be large to generate substantial radiation energy-density. Equation (8) is not strictly true at the start and end of the warm inflationary phase, as the stable radiation production condition will be violated.

In contrast the energy density of the inflaton during the slow-roll phase is dominated by its potential energy, giving

$$\rho_\phi = V(\phi). \quad (9)$$

The radiation density can be re-written as

$$\rho_\gamma = \frac{1}{12r} \left( \frac{V'}{H} \right)^2, \quad (10)$$

during warm inflation, since in the slow-roll phase the kinetic energy of the inflaton is controlled by the slope of the inflationary potential.

Introducing the dimensionless inflationary slow-roll parameter

$$\varepsilon \equiv \frac{m_p^2}{16\pi} \left( \frac{V'}{V} \right)^2 \quad (11)$$

we can relate the energy density of the radiation field to the energy-density of the inflaton by

$$\rho_\gamma = \left( \frac{\varepsilon}{2r} \right) \rho_\phi. \quad (12)$$

We have verified by numerical modelling (Section VI) that equation (12) holds very well during most of the warm inflationary phase.

We assume that warm inflation begins from a radiation dominated era, and starts when the energy density in the inflationary field is equal to that in the radiation field. Initially the radiation energy is redshifted away by the quasi-exponential expansion but enters a quasi-static phase when radiation production stabilises during the dissipation-dominated phase. Warm inflation ends when the universe heats up to become radiation dominated again, at a time when

$$\rho_\gamma = \rho_\phi. \quad (13)$$

At this epoch the universe stops inflating and smoothly enters a radiation dominated big-bang phase. This is one of the most attractive features of warm inflation, and suggests that its predictions are robust in the sense that they are not altered during the smooth transition to the radiation-dominated epoch. The material components of the universe are created by the decay of either the remaining inflationary field or the dominant radiation field.

The approximate relation, equation (12), and equation (13) suggest that an approximate condition for warm inflation to both begin and end is

$$\varepsilon = 2r, \quad (14)$$

although we do not expect this relation to be accurate since the condition of stable radiation production is violated at both epochs. In particular at the beginning of warm inflation the ambient radiation field is redshifted away during the sharp transition to warm inflation and the radiation density drops rapidly. Then at the end of the warm inflation phase, the production of radiation must end and we expect  $\dot{\rho}_\gamma \approx 3H\rho_\gamma \approx \Gamma\dot{\phi}^2$  during the turnover regime going from inflation-domination to radiation-domination.

In addition at both the beginning and end of warm inflation as the energy density of radiation is comparable to that of the inflationary potential, equation (3) should be used to describe the evolution of the universe rather than equation (4), introducing another approximation.

In Section VI we test the accuracy of our assumptions over the whole course of a warm inflationary phase by numerically integrating equations (1), (2) and (3) and find that for many models it appears that these approximations are accurate enough to be used to estimate the conditions over a large period of warm inflation, including the final few e-folds at the end of warm inflation.

The condition for a warm inflationary phase can be summarised by

$$\varepsilon < 2r. \quad (15)$$

It is straightforward to show that the same result can be derived from the requirement of accelerated expansion in the warm inflationary epoch. This requires that  $\ddot{a} > 0$  implying  $-\dot{H}/H^2 < 1$  or  $-\dot{\phi}H'(\phi)/H^2 < 1$ . Using equations (4) and (7) we again find the inequality of equation (15). The slow-roll condition and the additional strong dissipation condition

$$r > 1 \quad (16)$$

then implies warm inflation. One immediate consequence is that the usual inflationary condition,  $\varepsilon < 1$ , is no longer required as inflation (quasi-exponential expansion) can be maintained for steep potentials due to the damping of dissipation.

Finally, one can differentiate equation (7) with respect to time and, following from the slow-roll condition  $\dot{\phi} \ll V'$ , we find a constraint on the second derivative of the potential,

$$|\eta| \ll 3r^2 \quad (17)$$

where

$$\eta \equiv \frac{m_p^2 V''}{8\pi V} \quad (18)$$

is the curvature slow-roll parameter for inflation. This should be regarded as an extra condition for sustained warm inflation, and is a generalisation of the usual inflationary constraint,  $|\eta| \ll 1$ . Hence warm inflation can take place for a wider range of potentials than standard supercooled inflation.

### III. THE PERTURBATION SPECTRA

#### A. Adiabatic perturbations

Density perturbations are calculated in the same way as for standard inflation [12,14], via the equation

$$\delta_H = \frac{2}{5} \left( \frac{H}{\dot{\phi}} \right) \delta\phi, \quad (19)$$

where  $\dot{\phi}$  is given by equation (7). This equation holds for a mixture of inflationary and radiation fields, in the quasi-static regime of radiation production. It also can be shown that this result holds for any scalar field interacting adiabatically with another field, in the quasi-static limit, with the equation of state  $p = \omega\rho$ . In the presence of non-adiabatic perturbations (see Section III C) this relation does not necessarily hold. Specifically, if there non-adiabatic pressure perturbations, these can induce curvature perturbations to evolve on super-horizon scales [26]. However, we expect these effects to be small for the scenario discussed here and equation (19) can still be used for the order-of-magnitude estimates presented here.

The amplitude of perturbations,  $\delta_H$ , is related to the final dimensionless linear power spectrum of mass perturbations by

$$\Delta^2(k) = \left( \frac{k}{aH} \right)^4 T^2(k) \delta_H^2(k) \quad (20)$$

where  $T(k)$  is the matter transfer function relating initial spectra to the final, post-recombination linear spectra.

The fluctuations in the inflationary field are no longer generated by quantum fluctuations, but by thermal interactions with the radiation field;

$$\delta\phi^2 = \frac{k_F T}{2\pi^2}, \quad (21)$$

where  $k_F = \sqrt{\Gamma H} = \sqrt{3r}H \geq H$  is the freeze-out scale at which dissipation damps out the thermally excited fluctuations. The origin of the freeze-out wavenumber  $k_F$  is explained in Appendix A based on the original derivation in [14]. Note that in the warm inflationary epoch, the freeze-out length scale is generally much smaller than the Hubble radius. As one final point, when  $\Gamma \leq H$  and  $T \leq H$ , the amplitude of thermal fluctuations is equal to the amplitude of quantum fluctuations generated by Hawking radiation.

Combining equations (4), (7), (19) and (21) we find

$$\delta_H^2 = \frac{32}{75m_p^4} \frac{V}{\varepsilon} \left[ r^{5/2} \left( \frac{\sqrt{12}T}{H} \right) \right]. \quad (22)$$

The temperature of the radiation field is related to the potential by equations (8), (9) and (12) yielding

$$T^4 = \frac{\varepsilon V}{2r\alpha}. \quad (23)$$

Expressing the amplitude of density perturbations in terms of inflationary parameters we find

$$\delta_H^2 = \frac{16}{25\sqrt{\pi}m_p^3} \left( \frac{2}{\alpha} \left( \frac{r^3 V}{\varepsilon} \right)^3 \right)^{1/4}. \quad (24)$$

The ratio of thermal to quantum fluctuations is  $r^{5/2}T/H$ . During strong dissipation,  $r \gg 1$ , while towards the end of the warm inflationary era  $T/H \approx m_p/V^{1/4} \gg 1$ . Hence the thermal spectrum will dominate over the quantum spectrum of fluctuations during a warm inflationary phase.

### B. Spectral index of adiabatic perturbations

The spectral index of the adiabatic scalar perturbations is given by

$$n_s - 1 = \frac{d \ln \delta_H^2}{d \ln k} \quad (25)$$

where the logarithmic interval in wavenumber is related to the number of e-folds from the start of inflation,  $N(\phi)$ , and the scalar field by

$$d \ln k(\phi) = -dN(\phi) = -\frac{8\pi}{m_p^2} \frac{rV}{V'} d\phi. \quad (26)$$

Hence the spectral index of adiabatic density perturbations in warm inflation is given by

$$n_s = 1 - \frac{3}{4r}(3\varepsilon - 2\eta). \quad (27)$$

As we require that  $r \gg 1$  we expect the deviation from scale invariance to be suppressed in the warm inflationary model, until  $\varepsilon \approx r$ , at the end of the warm inflation phase. If  $\varepsilon > (2/3)\eta$ , or  $\eta$  is negative, the spectrum of adiabatic fluctuations will be red, with the spectrum suppressed on small scales, as in standard supercooled inflation which generally also produces slopes  $n_s \leq 1$ . However, in the opposite case, when  $\varepsilon < (2/3)\eta$ , the spectrum of adiabatic fluctuations will be blue, in contrast with predictions from generic standard inflation models. With a blue spectrum, the interesting possibility exists of producing primordial black holes on small scales [27].

### C. Isocurvature perturbations

Isocurvature perturbations also are generated in the warm inflationary era due to thermal fluctuations in the radiation field. These perturbations can be characterised by fluctuations in the entropy,  $S_X$ , where the species  $X$

is undergoing thermal fluctuations relative to the number density of photons

$$S_X = \frac{3}{4}(\delta_X - \delta_\gamma) \quad (28)$$

and we have assumed the  $X$ -field is the ambient radiation field excluding photons.

Assuming that the isocurvature fluctuations are thermal in origin, their perturbation spectrum is

$$\begin{aligned} \delta_{\text{iso}}^2 &= \frac{1}{25m_p^2} \frac{k_F T}{2\pi^2} \\ &= \frac{1}{25\sqrt{\pi^3}} \left( \frac{2r\varepsilon}{\alpha} \right)^{1/4} \left( \frac{V^{1/4}}{m_p} \right)^3. \end{aligned} \quad (29)$$

This relation is true only for non-interacting fields, but again should hold for order-of-magnitude estimates. The ratio of isocurvature to adiabatic perturbations is

$$R_{\text{iso}} \equiv \frac{\delta_{\text{iso}}^2}{\delta_H^2} = \frac{\varepsilon}{16\pi r^2} \quad (30)$$

so that when  $r \gg 1$  and  $r \geq \varepsilon$  adiabatic perturbations will dominate. In practice the scalar modes will form a quadratic sum of adiabatic and isocurvature modes,

$$\delta_s^2 = \delta_H^2 + \delta_{\text{iso}}^2, \quad (31)$$

and which can be separated observationally since isocurvature generated fluctuations of the CMB are out of phase with adiabatic perturbations. Another discriminator is if super-horizon perturbations can be observed, for instance in the CMB [28]. Since isocurvature modes do not contribute to curvature perturbations (in the comoving gauge) the contribution from isocurvature modes should be absent from super-horizon perturbations, leading to a drop in amplitude of the scalar perturbations at the horizon scale. Isocurvature perturbations have previously been discussed in the context of warm inflation by [29], although no detailed calculation of their amplitude was given.

### D. Spectral index of isocurvature perturbations

Following the derivation of the spectral index of adiabatic perturbation, the spectral index of the isocurvature perturbations, defined by

$$n_{\text{iso}} \equiv \frac{d \ln \delta_{\text{iso}}^2}{d \ln k}, \quad (32)$$

is

$$n_{\text{iso}} = -\frac{1}{4r}(\varepsilon + 2\eta). \quad (33)$$

This differs from isocurvature fluctuations generated by quantum fluctuations, where  $n_{\text{iso}} = -2\varepsilon$ . If  $r$  is large, the spectrum will again tend to be flat, until  $\varepsilon \approx r$ . If  $\varepsilon > -2\eta$  the thermal isocurvature spectrum will be red as it is in standard supercooled inflation.

## E. Tensor perturbations

Tensor perturbations do not couple strongly to the thermal background and so gravitational waves are only generated by quantum fluctuations, as in standard supercooled inflation. Their spectrum is given by [25]

$$A_g^2 = \frac{32V}{75m_p^4}, \quad (34)$$

with spectral index

$$n_g \equiv \frac{d \ln A_g^2}{d \ln k} = -\frac{2\varepsilon}{r}, \quad (35)$$

and the inequality  $-4 < n_g < 0$  arising from the warm inflation condition  $\varepsilon \leq r$ .

The ratio of tensor to scalar perturbations is

$$R_g \equiv \frac{A_g^2}{\delta_H^2} = \frac{\sqrt{\pi}}{3} \left( \frac{2\varepsilon}{r^3} \right)^{3/4} \left( \frac{\alpha V}{m_p^4} \right)^{1/4}. \quad (36)$$

Hence, as we are in the strongly dissipative regime, where  $r \gg 1$  and  $\varepsilon \leq r$ , we expect the contribution from gravitational waves to be small unless the magnitude of the potential is large or  $r$  is order unity.

The ratio of the amplitude of isocurvature to tensor perturbations scales as

$$\frac{\delta_{\text{iso}}^2}{A_g^2} = \frac{3m_p}{32\sqrt{\pi^3}} \left( \frac{2r\varepsilon}{\alpha V} \right)^{1/4}, \quad (37)$$

which will be greater than unity unless the scale of the potential is large. Hence we can expect that the inequalities

$$R_g < R_{\text{iso}} < 1 \quad (38)$$

in general will hold. We find that this is true for all the of the numerical models we consider in Sections V and VI.

## F. Comparison with Standard Supercooled Inflation

A nice feature of warm inflation is that these results are significantly different from standard supercooled inflation case, where

$$\begin{aligned} \delta_H^2 &= \frac{32V}{75m_p^4\varepsilon}, \\ n_s &= 1 - 6\varepsilon + 2\eta, \\ n_g &= -2\varepsilon, \\ R_g &= \varepsilon. \end{aligned} \quad (39)$$

Thus near future observations should be able to distinguish between the two. An immediate consequence of our analysis is that there need be no consistency relationship between the scalar spectral index and the ratio of tensor to scalar perturbations, as in standard inflation. We discuss the observational differences between the models in Section VII.

## IV. CONDITIONS AT THE END OF INFLATION

At the end of the warm inflationary epoch, the dissipation parameter,  $r$ , is related to the slow-roll parameter,  $\varepsilon$ , by equation (14). Substituting in equations (6), (4) and (11) we form a differential equation which can be solved for  $V(\phi)$  to find the magnitude of the potential field at the end of warm inflation,

$$V(\phi_{\text{end}}) = \frac{\pi}{6} \left( \frac{\Gamma}{m_p} \right)^2 \phi_{\text{end}}^4, \quad (40)$$

up to a constant, but independent of the shape of the inflationary potential. This selects out the  $V \approx \phi^4$  potential as a special case where warm inflation never ends (see Appendix B). This is due to the energy density of the radiation field “tracking” the energy density in the inflationary field,  $\rho_\gamma \propto \rho_\phi$ , and so the condition for warm inflation to end is never met. In this case warm inflation continues until the slow-roll conditions are no longer met and the inflaton field decays away, which then ends inflation. For  $n > 4$  and exponential potentials, the radiation density will always fall faster than the energy-density of the inflaton field (see Appendix B). In this case warm inflation will occur, in the sense that a sizable radiation component can persist for a considerable duration during inflation, well beyond the requirements for solving the problems of standard cosmology. However to end such a warm inflation regime, this behavior of the potential must be local, and at some point the vacuum energy must be released at a sufficiently fast rate to allow the radiation to dominate.

## V. SPECIFIC CASES

In order to understand how warm inflation differs from the standard supercooled inflationary scenario, it is useful to consider a few specific examples. Here we consider models of warm inflation with polynomial and exponential potentials.

### A. Polynomial inflation

We consider the simplest inflationary model

$$V(\phi) = m^2\phi^2/2 \quad (41)$$

for a massive scalar field with mass  $m$ . With this potential the slow-roll parameters are

$$\varepsilon = \eta = \frac{m_p^2}{4\pi\phi^2}. \quad (42)$$

The Hubble parameter is given by

$$H(\phi) = \sqrt{\frac{4\pi}{3}} \left( \frac{m}{m_p} \right) \phi \quad (43)$$

while the dissipation parameter scales like

$$r = \frac{1}{\sqrt{12\pi}} \left( \frac{\Gamma}{m} \right) \frac{m_p}{\phi}. \quad (44)$$

From equation (44) we see that the ratio  $\Gamma/m$  controls the evolution of the system.

Solving equation (7) we find that the inflaton field evolves as

$$\begin{aligned} \phi(t) &= \phi_0 e^{-m^2 t/\Gamma} \\ &\approx \phi_0 \left( 1 - \frac{m^2}{\Gamma} t \right). \end{aligned} \quad (45)$$

Compared with standard inflation, where [5]

$$\phi(t) \approx \phi_0 - \left( \frac{m m_p}{\sqrt{12\pi}} \right) t, \quad (46)$$

we see that during warm inflation the inflaton field decays due to dissipation into the radiation field.

The energy densities of the inflationary potential is given by equation (9) and (41) while the radiation field is given by

$$\rho_\gamma = \sqrt{\frac{3}{\pi}} \left( \frac{m^3 m_p}{8\Gamma} \right) \phi = \sqrt{\frac{6}{\pi}} \left( \frac{m^2 m_p}{8\Gamma} \right) \rho_\phi^{1/2}. \quad (47)$$

The number of e-folds from the end of warm inflation is given by

$$\begin{aligned} N(\phi) &= -\ln k(\phi) \\ &= -\frac{8\pi}{m_p^2} \int_\phi^{\phi_{\text{end}}} d\phi' \frac{rV}{V'} \\ &= \sqrt{\frac{4\pi}{3}} \left( \frac{\Gamma}{m} \right) \frac{1}{m_p} (\phi - \phi_{\text{end}}). \end{aligned} \quad (48)$$

Figure 1 shows the evolution of the energy densities of the radiation and inflationary fields as a function of number of e-folds. The upper line is the inflation energy density and the lower line the radiation energy density. The dashed lines are the results of our analytic model, from equations (41), (47) and (50), while the solid lines are the results of our numerical model (Section VI) of the evolution of the field through the warm inflationary era.

From the condition that  $\varepsilon = 2r$  at the end of warm inflation we find that the magnitude of the inflationary field at this time is

$$\phi_{\text{end}} = \frac{1}{2} \sqrt{\frac{3}{4\pi}} m_p \left( \frac{m}{\Gamma} \right) \quad (49)$$

where the initial field must have  $|\phi_0| > \phi_{\text{end}}$ . In standard polynomial ( $n = 2$ ) inflation this condition is  $|\phi|_{\text{end}} > m_p/\sqrt{4\pi}$ , so we find that for warm inflation this is weakened by the factor  $\approx m/\Gamma$ . If  $\Gamma > m$  then warm inflation can begin well below the Planck mass.

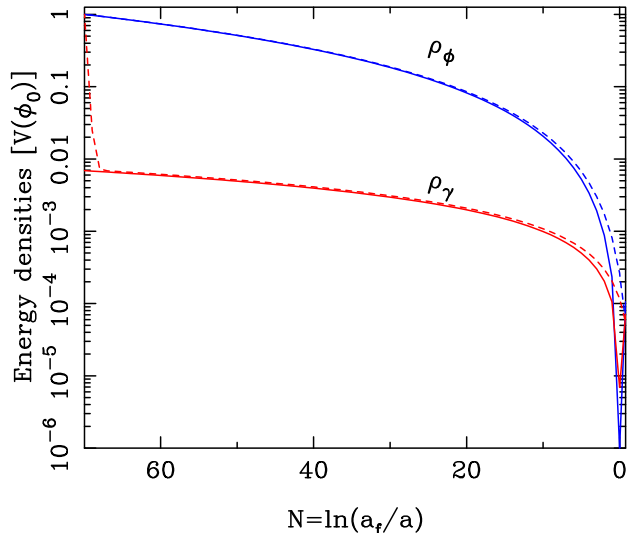


FIG. 1. The evolution of energy density of the inflationary and radiation fields as a function of number of e-folds from the end of warm inflation,  $N = \ln(a_f/a)$ , where  $a_f$  is the final expansion factor, for the inflationary potential  $V = m^2\phi^2/2$ . The energy-density of the inflationary field (upper curves) and the radiation field (lower curves) are both normalised to unity in units of the magnitude of the potential at the start of inflation,  $V(\phi_0)$ . The solid lines are the results of the analytic expressions equations (47), while the dashed lines are the results of the numerical model discussed in Section VI.

The total number of e-folds from the end of warm inflation is

$$N_{\text{tot}} = \sqrt{\frac{4\pi}{3}} \left( \frac{\Gamma}{m} \right) \left( \frac{\phi_0}{m_p} \right) - \frac{1}{2}. \quad (50)$$

As we require  $N \approx 70$  e-folds to comfortably solve the problems of standard cosmology this implies

$$\phi_0 \approx 35 \left( \frac{m}{\Gamma} \right) m_p. \quad (51)$$

The requirement of strong dissipation also leads to a constraint on  $\Gamma$ . From equation (44) with equation (51) we find that at the beginning of inflation

$$r(\phi_0) \approx \frac{1}{215} \left( \frac{\Gamma}{m} \right)^2 \gg 1 \quad (52)$$

resulting in the requirement that  $\Gamma \gg 15m$  for warm inflation to commence in polynomial ( $n = 2$ ) inflation.

Calculating the spectrum of adiabatic perturbations yields

$$\delta_H^2 = \frac{2}{75} \left( \frac{2}{3\alpha\pi^5} \right)^{1/4} \left( \frac{\Gamma}{m_p} \right)^{3/2} \left( \ln \frac{k}{k_{\text{end}}} \right)^{3/4}, \quad (53)$$

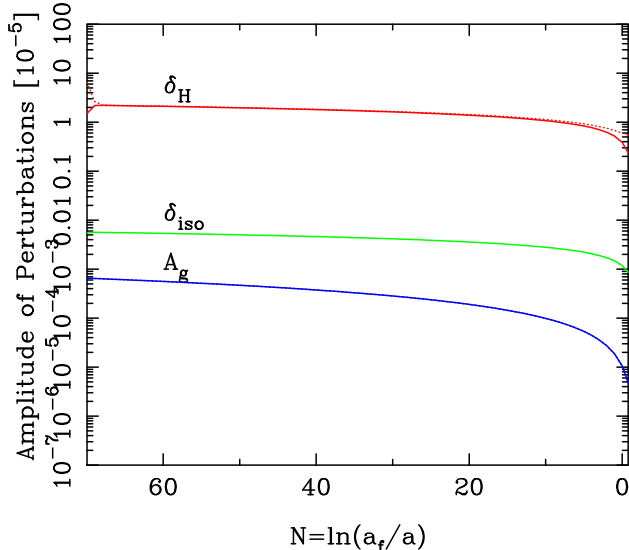


FIG. 2. The perturbation spectra of adiabatic scalar perturbations (top line), isocurvature scalar perturbations (middle line) and gravitational waves (bottom line) as a function of e-folds from the end of warm inflation,  $N$ , for the potential  $V = m^2 \phi^2/2$ . The model is normalised to have  $\delta_H = 2 \times 10^{-5}$  at the 50<sup>th</sup> e-fold. Solid lines are the results of our analytical model, while the dotted lines are from the numerical model.

where  $\ln k_{\text{end}} = \sqrt{4\pi/3}\Gamma\phi_{\text{end}}/(mm_p) \approx 1/2$  is the fiducial wavenumber at the end of warm inflation. Note that the amplitude of adiabatic perturbations is independent of the magnitude of the inflationary potential. In Appendix B we show that the amplitude of adiabatic perturbations in warm inflation is independent of the magnitude of the inflationary potential for all polynomial potentials.

Figure 2 shows the amplitude of adiabatic, isocurvature and tensor perturbations for the  $n = 2$  polynomial. In Appendix B we derive results for the more general polynomial and exponential cases. We find that the ratio of the amplitude of perturbations agrees with the inequality expressed by equation (38). For the  $n = 2$  case the isocurvature and tensor perturbations are strongly suppressed below the adiabatic perturbations. This difference can be reduced by increasing the magnitude of the inflationary potential.

The spectral indices are related by

$$n_s - 1 = n_{\text{iso}} = \frac{3}{8}n_g = -\frac{3\varepsilon}{4r}, \quad (54)$$

and are all red. In Appendix B we derive more results for the general case of  $\phi^n$  potentials. There we show that for polynomial potentials the spectral index is always red unless  $n > 4$ , or for the case of an exponential potential (see Appendix B), in which case the spectrum is blue. The latter open up the interesting possibility of primordial black hole production in the early universe [27]. A

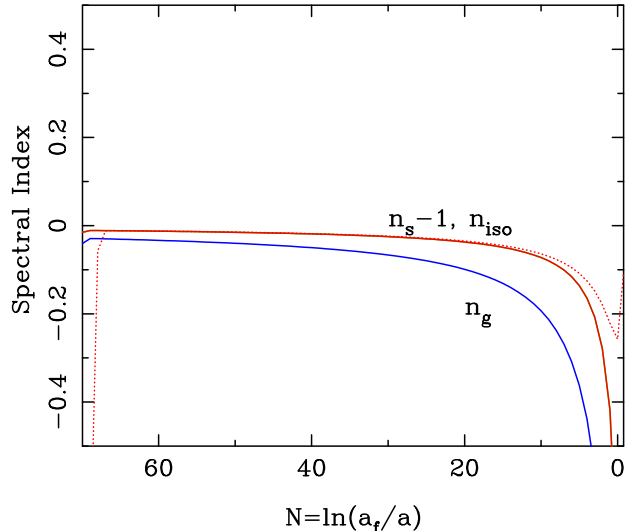


FIG. 3. The spectral indices of the adiabatic scalar perturbations,  $n_s - 1$ , isocurvature scalar perturbations,  $n_{\text{iso}}$ , and gravitational waves,  $n_g$ , as a function of e-folds from the end of warm inflation,  $N$ , for the potential  $V = m^2 \phi^2/2$ . The solid lines are for our analytical model, while dotted lines are from the numerical model. The spectral index of the isocurvature perturbations lies under that of the adiabatic curve.

scale invariant spectrum,  $n_s = 1$ , is found only for the  $n = 4$  model.

The dissipation ratio,  $r$ , and the slow-roll parameter  $\varepsilon$  are related by

$$r = \frac{1}{\sqrt{3}} \left( \frac{\Gamma}{m} \right) \varepsilon^{1/2} \quad (55)$$

so that the ratio of isocurvature to adiabatic perturbations, given by  $\varepsilon/r^2$ , is  $3(m/\Gamma)^2 \ll 1$ .

Figure 3 shows the spectral indices of the adiabatic, isocurvature and tensor spectra as a function of wavenumber. In all cases the spectral indices starts as a flat spectrum, when  $\varepsilon \ll r$ . In the case of  $n = 4$  spectral indices are exactly flat while for the exponential potential the spectral indices are almost flat.

## VI. NUMERICAL MODELS

While our analytic results simplify the whole analysis of warm inflationary models, it is important to verify the range of validity of this analysis and find where the assumptions used in their derivation are accurate. To test this we have numerically evolved the inflationary and radiation fields through a warm inflationary epoch, and calculated the adiabatic and tensor perturbation spectra. We numerically solve equations (1) and (2) for the evolution of the field and equation (3) for the evolution of the background universe using the methods of [20].

The results for the evolution of the energy-density of the fields for the case of a polynomial  $n = 2$  potential are shown in Figure 1. The magnitude of the inflationary and radiation energy-density fields are both normalised to unity in units of the potential at the start of inflation. We set  $\rho_\gamma = \rho_\phi$  initially, as it is reasonable to assume that inflation begins from a radiation-dominated epoch. We tested a number of other initial conditions including  $\rho_\gamma = 0$  and found little variation in our final results, as the models soon settled down to the same evolution after the first few e-folds.

To parameterise the models we used the more general expression for polynomial inflation from Appendix B, and choose parameters so that the amplitude of adiabatic perturbations  $\delta_H = 2 \times 10^{-5}$  at the  $50^{th}$  e-fold, and allowed a total of 70 e-folds of warm inflation to elapse.

Figure 1 verifies that not only the shapes of the curves are well approximated, but also the relative magnitudes of the radiation and inflationary energy-densities are accurately reproduced. The main assumptions underlying our analytic results are that of slow-roll inflation and quasi-stable radiation production ( $\dot{\rho}_\gamma \ll \Gamma \dot{\phi}^2$ ). The latter assumption breaks down at the start of warm inflation as the radiation field initially is redshifted away. But radiation production by dissipation of the inflaton field soon catches up with the redshifting and stability is reached after a few e-folds.

We found accurate agreement between our analytic models and the full numerical models for polynomial potentials in the range  $0.5 < n < 4$ . In most cases the agreement was  $< 1\%$  over most of the range, except near the beginning of inflation. In the  $n = 4$  case the energy densities tracked each other as expected from our discussion in Section IV. We also tested our results for the exponential potential discussed in Appendix B, and again found similar accuracy, although here again the radiation field drops faster than the energy density in the inflationary field and warm inflation has to end by the natural decay of the inflaton, or by some other means.

We have also computed the amplitude and scale dependence of the perturbation spectra for adiabatic perturbations directly from equations (19) and (21). These are plotted for the case of  $n = 2$  in Figure 2. Again close agreement was found, with deviations less than 1% over the range of wavenumbers. Again the poorest agreement was over the few e-folds at the beginning and end of warm inflation.

Finally we tested the predicted spectral indices for adiabatic perturbations (Fig. 3). Again we found good agreement between the analytic and numerical models, except for the first and last few e-folds. The sudden change in  $n_s - 1$  at the beginning of warm inflation ( $N \approx 70$ ) is real and due to the sharp transition to warm inflation when the change in the radiation density,  $\dot{\rho}_\gamma$ , is important.

## VII. OBSERVATIONAL CONSTRAINTS

In standard inflation, there are four observable constraints ( $\delta_H, A_g, n_s, n_g$ ) for the three parameters of slow-roll inflation,  $V_0, \varepsilon, \eta$ , where  $V_0$  is the magnitude of the inflationary potential. With four constraints there is a redundancy in the observations allowing a consistency relation [25]. This is usually expressed as a relationship between the tensor-to-scalar ratio and the slope of the tensor spectrum,

$$R_g = -\frac{n_g}{2}. \quad (56)$$

This appears to be generally true for slow-roll inflation, although recent work on pre-heating at the end of supercooled inflation may effect this result [8–11].

In warm inflation the dissipation factor,  $r$ , becomes an active parameter (since it is present at the end of supercooled inflation, but assumed inactive) giving four constraints for four parameters. Hence we do not expect the consistency relation of standard inflation to hold in warm inflation. This relation can only arise by coincidence. If the consistency relation is not observed it may indicate a warm inflationary phase. The dissipation factor can be estimated from the observables by the relation

$$r^2 \approx -n_g \left( \frac{25\alpha\pi^2}{32} R_g^4 A_g^2 \right)^{1/3}. \quad (57)$$

To discriminate between warm and standard inflation requires a measurement of all four observables. The MAP and Planck satellite missions will probe the CMB and provide strong constraints on the amplitude and shape of the scalar perturbation spectrum. Both MAP and Planck have polarisation detectors which are sensitive to tensor modes, but Planck has a much broader range of frequencies which will aid the subtraction of foreground contamination of the CMB signal. In practice the tensor modes may be so small as to be unobservable, hence it may not be easy to distinguish between the two models.

Current observations, from the COBE satellite, and subsequent airborne detectors (see [30] for a recent analysis), can be used to place constraints on the amplitude of scalar perturbations and the slope of their spectra. The low COBE multipoles indicate that  $\delta_H^2 \approx 10^{-10}$ , giving the constraint

$$\begin{aligned} V^{1/4} &\approx 7.6 \times 10^{-4} (\alpha^{1/3} \varepsilon r^{-3})^{1/4} m_p, \\ &\approx 7.6 \times 10^{15} (\alpha^{1/3} \varepsilon r^{-3})^{1/4} \text{GeV}. \end{aligned} \quad (58)$$

If  $r^3 \approx \alpha^{1/3} \varepsilon$ , these energy scales are pretty much in keeping with those of Grand Unified Theories. However if  $r \gg 1$  as required for warm inflation we open up the interesting possibility that the energy scale required can be much lower.



## VIII. CONCLUSIONS

In this paper we have investigated the phenomenology of the warm inflationary scenario. In the slow-roll, warm inflation epoch we have found the general relationship between the energy-density in the inflaton and radiation fields. This has led us to the general criteria for warm inflation,  $\varepsilon < r$ ,  $|\eta| < 3r^2$  and  $r > 1$ . The usual inflation condition,  $\varepsilon < 1$ , is generalised as dissipation can help sustain accelerated expansion of the universe for a wider range of inflationary potentials.

Generalising the analysis of inflation in the slow-roll regime, we have derived expressions for the perturbation spectra of adiabatic and isocurvature fluctuations generated by thermal fluctuations during the warm inflationary epoch. The adiabatic spectrum produced by thermal fluctuations dominates that produced by quantum fluctuation. Its amplitude and spectral slope are both different from quantum generated perturbations and can lead to red or blue spectra. Isocurvature perturbations also are generated due to internal fluctuation between radiation fields. These are generally suppressed compared to the adiabatic spectrum.

Gravitational waves are still generated via quantum excitation, and have the same amplitude but different slope from standard inflation. The tensor-to-scalar ratio is suppressed by the relatively high amplitude of the adiabatic spectrum.

No consistency relation exists in warm inflation as there are now four parameters (the standard three of inflation and an active dissipation factor) and in general only four observables. This is probably the most important observational test of warm inflation, but may be difficult, even for Planck, if the tensor modes are strongly suppressed. In this case measurement of the isocurvature modes relative to adiabatic would provide an alternative test. However, verification of the consistency relation would rule out substantial interactions during inflation.

There are two important differences between standard and warm inflation. First, the slope of the inflationary potential does not need to be small, as dissipation will allow slow-roll even for steep potentials. Second, the energy scale of warm inflation may be much lower than required for standard inflation, due to the higher amplitude of thermal adiabatic perturbations and the constraints of Sachs-Wolfe effects observed in the CMB.

To investigate the warm inflationary model we need to study further the evolution of scalar perturbations during the transition phase from warm inflation to radiation domination when the energy densities of the radiation field and inflationary field are comparable. This will occur more smoothly than in standard inflation and should lead to observational differences between the models. In addition the model we have presented here for isocurvature perturbations is crude. A more complete understanding of the generic prediction of isocurvature perturbations for warm inflation is needed before detailed

predictions can be made.

The model we have presented here is an extreme one, in that we have assumed that it is dissipation-dominated. A whole range of models lie between that of warm inflation and the standard supercooled inflation, and it would be interesting to explore their properties in the general framework we have outlined here. The development in [19] also would be beneficial for this.

Finally these results should be propagated to the post-recombination era using general-purpose transfer codes such as CMBfast [31]. However to make definite, high-quality predictions for the CMB, such codes must be generalised to remove any of the relations of standard supercooled inflation, such as the consistency relation. This will allow us to predict with some confidence whether the MAP and Planck missions will be able to probe the high redshift universe with sufficient accuracy to distinguish between warm and supercooled inflation.

Acknowledgements: ANT and AB acknowledge the support of PPARC, and thank David Wands for useful discussion about the evolution of non-adiabatic super-horizon perturbations.

## APPENDIX A

The origin of the “freeze-out” wavenumber  $k_F$  in equation (21) is reviewed here following the original and more detailed explanation in [14]. To account for fluctuations, the inflaton now is written as  $\phi(\mathbf{x}, t) = \phi_0(t) + \delta\phi(\mathbf{x}, t)$ . Assuming the universe remains near thermal equilibrium during warm inflation, the fluctuations of the inflaton field obey a fluctuation-dissipation relation. The evolution equation for the fluctuations,  $\delta\phi(\mathbf{x}, t)$ , is obtained from the linearized deviation of the zero mode equation of motion equation (1), with inclusion of the spatial Laplacian term and the addition of a white-noise random force term

$$\Gamma \frac{d\delta\phi(\mathbf{k}, t)}{dt} = -[\mathbf{k}^2 + V''(\phi_0)]\delta\phi(\mathbf{k}, t) + \xi(\mathbf{k}, t), \quad (59)$$

where  $V''(\phi_0) = d^2V(\phi_0)/d\phi_0^2$  and we have Fourier transformed to momentum space. The white-noise represents the action of the thermal heat bath on the inflaton field, with the spectrum of the this noise term governed by the fluctuation-dissipation theorem,

$$\langle \xi(\mathbf{k}, t) \rangle = 0 \quad (60)$$

and

$$\langle \xi(\mathbf{k}, t) \xi(-\mathbf{k}', t') \rangle_\xi \stackrel{T \rightarrow \infty}{=} 2\Gamma T (2\pi)^3 \delta^{(3)}(\mathbf{k} - \mathbf{k}') \delta(t - t'). \quad (61)$$

The solution of equation (59) is

$$\begin{aligned} \delta\phi(\mathbf{k}, t) \approx & \frac{1}{\Gamma} e^{-(t-t_0)/\tau(\phi)} \int_{t_0}^t e^{(t'-t_0)/\tau(\phi_0)} \xi(\mathbf{k}, t') dt' \\ & + \delta\phi(\mathbf{k}, t_0) e^{-(t-t_0)/\tau(\phi_0)}, \end{aligned} \quad (62)$$

where  $\tau(\phi) = \Gamma/(k^2 + V''(\phi))$ . The first term on the right hand side acts to thermalize  $\delta\phi$ , whereas the latter is the memory term for the initial value of  $\delta\phi$ , which over time becomes negligible.

In the cosmological case, equation (59) must be interpreted for physical wavenumbers, since the thermal effects as expressed in this equation act in accordance with the physical wavenumbers of the system. Thus for a given fluctuation mode,  $\delta\phi(\mathbf{k}_c)$ , at comoving wavenumber  $\mathbf{k}_c$ , equation (59) expresses its dynamics within the time interval  $1/H$  when the physical mode is  $k_{phys} \equiv k_c e^{-Ht} \approx k$ . To be consistent with the thermalization conditions, during the time interval  $\sim 1/H$  the mode  $\phi(\mathbf{k}_c)$  must thermalize at physical scale  $k$ . In terms of the solution equation (62), this requires the memory term to be negligible within a Hubble time, thus

$$\frac{k^2 + V''(\phi_0)}{H\Gamma} > 1. \quad (63)$$

The freeze-out wavenumber  $k_F$  is at the point where this condition first holds, which for  $V''(\phi_0) < \Gamma H$  is

$$k_F = \sqrt{\Gamma H}. \quad (64)$$

If  $V''(\phi_0) > H\Gamma$  then the freeze-out wavenumber is the same as for supercooled inflation,  $k_F = H$ . However, in general this regime never occurs during warm inflation and equation (64) is the governing condition. Note that  $H$  varies during warm inflation, thus based on equation (64), so too will  $k_F$ . However, the variation of  $H$  is typically very small, less than a factor 10, during the entire warm inflation period. Thus, up to order one factors, one can treat  $k_F$  as a constant with  $H$  evaluated at some appropriate time during warm inflation, such as the beginning. In our analytic approach we have included the  $\phi$ -dependence of  $k_F$ .

In our treatment here we have taken the dissipative coefficient  $\Gamma$  to be independent of  $k$ , whereas in [14] it was mentioned that in general  $\Gamma$  will depend on  $k$  and generally will decrease with increasing wavenumber. In this case, the condition equation (64) still is valid except it must now be solved for  $k_F$  due to the  $k$ -dependence in  $\Gamma$ .

## APPENDIX B

### Polynomial potentials

In this appendix we explore the properties of the warm inflationary scenario for the family of models with the functional form

$$V(\phi) = \lambda m^4 \left(\frac{\phi}{m}\right)^n \quad (65)$$

where  $\lambda$  is a dimensionless parameter, which allows more freedom in the normalisation of the potential.

The slow-roll parameters are given by

$$\varepsilon = \frac{n^2 m_p^2}{16\pi\phi^2}, \quad \eta = \frac{n(n-1)m_p^2}{8\pi\phi^2} \quad (66)$$

with the relation

$$\varepsilon = \frac{n}{2(n-1)}\eta. \quad (67)$$

The expansion of the universe is governed by the Hubble parameter

$$H(\phi) = \sqrt{\frac{8\pi\lambda}{3}} \frac{m^2}{m_p} \left(\frac{\phi}{m}\right)^{n/2}, \quad (68)$$

where the dimensionless dissipation parameter is

$$r = \frac{1}{\sqrt{24\pi\lambda}} \left(\frac{\Gamma}{m}\right) \left(\frac{m_p}{m}\right) \left(\frac{\phi}{m}\right)^{-n/2}. \quad (69)$$

The energy density of the radiation field is given by

$$\rho_\gamma = \sqrt{\frac{3\lambda^3}{2\pi}} \frac{n^2 m_p}{8 \Gamma} m^4 \left(\frac{m}{\phi}\right)^{(4-3n)/2}, \quad (70)$$

and related to the energy-density of the inflation field by

$$\rho_\gamma = \sqrt{\frac{3}{2\pi}} \frac{n^2 m_p}{8 \Gamma} m_p^4 \left[ \lambda \left(\frac{m}{m_p}\right)^{4-n} \right]^{2/n} \left(\frac{2\rho_\phi}{m_p^4}\right)^{\frac{(3n-4)}{2n}}. \quad (71)$$

This last relation tells us that for an  $n = 4$  potential the energy densities are proportional,  $\rho_\gamma \propto \rho_\phi$ , and that warm inflation cannot end by the condition given by equation (14). When the potential is steeper than this,  $n > 4$ , or for the exponential potential, the radiation field drops more rapidly than the inflation field. Although warm inflation occurs, the effects of the radiation field will diminish and inflation will begin to evolve in the same way as for standard inflation. Hence for polynomial inflationary potentials we require  $n < 4$  for strong warm inflation to take hold.

The number of e-folds,  $N(\phi)$ , the universe expands during inflation is

$$N(\phi) = \sqrt{\frac{2\pi}{3\lambda}} \frac{8\Gamma}{n(4-n)m_p} \left[ \left(\frac{\phi_0}{m}\right)^{\frac{(4-n)}{2}} - \left(\frac{\phi}{m}\right)^{\frac{(4-n)}{2}} \right] \quad (72)$$

where we count the number of e-folds from the start of warm inflation (note in Section V we counted e-folds from the end of warm inflation). The number of e-folds can be related to  $\varepsilon$  and  $r$  by

$$N(\phi) = \left(\frac{2n}{4-n}\right) \left(\frac{r_0}{\varepsilon_0} - \frac{r}{\varepsilon}\right). \quad (73)$$

If  $n < 4$  then  $N$  is dominated by the ratio of  $\varepsilon/r$  at the start of the inflationary phase, and to a good approximation the total number of e-folds is

$$N_{\text{tot}} = \left( \frac{2n}{4-n} \right) \frac{r_0}{\varepsilon_0}. \quad (74)$$

The adiabatic spectrum of density perturbations is

$$\delta_H^2 = \frac{8}{75} \left( \frac{2^7}{3^5 \pi^7 \lambda^3} \right)^{1/8} \left( \frac{\Gamma^9}{\alpha n^6 m_p^9} \right)^{1/4} \left( \frac{\phi}{m} \right)^{3(4-n)/8}. \quad (75)$$

Substituting in equation (72) we find that the amplitude of adiabatic perturbations in warm inflation is independent of the magnitude of the inflationary potential for polynomial potentials, when expressed as a function of e-folds, or scale.

The spectral index of adiabatic fluctuations is related to the slow-roll parameter,  $\varepsilon$ , and the dissipation parameter,  $r$ , by

$$n_s - 1 = -\frac{(4-n)3\varepsilon}{n4r} = \frac{(4-n)3}{n8} n_g = \frac{3(4-n)}{(5n-4)} n_{\text{iso}}. \quad (76)$$

where the last two expressions relate the adiabatic spectral index to the isocurvature and tensor spectral index. From this expression we see that the warm inflationary adiabatic spectrum is only exactly scale invariant ( $n_s = 1$ ) for potentials with  $n = 4$ , and is red unless  $n > 4$ .

The isocurvature spectrum is given by

$$\delta_{\text{iso}}^2 = \frac{1}{50} \left( \frac{\lambda^5}{6^3 \pi^{15}} \right)^{1/8} \left( \frac{m}{m_p} \right)^2 \left[ \frac{n^2}{\alpha} \frac{\Gamma}{m_p} \left( \frac{\phi}{m} \right)^{(5n-4)/2} \right]^{1/4}. \quad (77)$$

The ratio of the amplitude of isocurvature to adiabatic perturbations is given by

$$R_I = \frac{\varepsilon}{16\pi r^2} = \frac{3\lambda n^2}{32\pi} \left( \frac{m}{\Gamma} \right)^2 \left( \frac{\phi}{m} \right)^{n-2}. \quad (78)$$

In the special case of  $n = 2$  this is a constant, as found in Section V.

### Exponential potential

Consider potentials of the form

$$V(\phi) = V_0 \exp \frac{\phi}{\kappa}, \quad (79)$$

where  $\kappa$  is a free parameter with units of mass.

The slow-roll parameters are

$$\eta = 2\varepsilon = \frac{m_p^2}{8\pi\kappa^2}. \quad (80)$$

The energy densities of the radiation and inflationary fields are related by

$$\rho_\gamma = \sqrt{\frac{3}{2\pi}} \left( \frac{m_p}{8\Gamma\kappa^2} \right) \rho_\phi^{3/2}. \quad (81)$$

Hence the energy density of the radiation field falls more rapidly than that of the inflationary field, as predicted. In the exponential model, warm inflation will end in the same way as discussed earlier for  $n > 4$  polynomial potentials.

The number of e-folds from the start of warm inflation is

$$\begin{aligned} N(\phi) &= \sqrt{\frac{2\pi}{3}} \left( \frac{4\Gamma\kappa^2}{m_p} \right) (V^{-1/2}(\phi_0) - V^{-1/2}(\phi)) \\ &= \left( \left( \frac{r}{\varepsilon} \right)_0 - \left( \frac{r}{\varepsilon} \right)_\phi \right). \end{aligned} \quad (82)$$

The amplitude of adiabatic scalar perturbations is

$$\delta_H^2 = \frac{8}{75} \left( \frac{2}{\pi} \right)^{7/8} \frac{1}{3^{5/8} \alpha^{1/4}} \left( \frac{\kappa}{m_p} \right)^{3/2} \left( \frac{\Gamma}{m_p} \right)^{9/4} \left( \frac{V}{m_p^4} \right)^{-3/8} \quad (83)$$

while that of isocurvature perturbations is given by

$$\delta_{\text{iso}}^2 = \frac{1}{50} (6^3 \pi^{15})^{1/8} \left( \frac{\Gamma}{m_p} \right) \left( \frac{m_p^2}{a\kappa^2} \right)^{1/4} \left( \frac{V}{m_p^4} \right)^{5/8} \quad (84)$$

with ratio

$$R_{\text{iso}} = \frac{9\pi^{11/4}}{16\sqrt{2}} \left( \frac{\Gamma}{m_p} \right)^{-2} \left( \frac{m_p}{\kappa} \right)^2 \left( \frac{V}{m_p} \right). \quad (85)$$

The adiabatic and isocurvature spectral indices are

$$n_s - 1 = \frac{3\varepsilon}{4r}, \quad n_{\text{iso}} = -\frac{5\varepsilon}{4r}. \quad (86)$$

For warm inflation with an exponential potential, the adiabatic spectrum is always blue in contrast with standard inflation while the isocurvature is always red. The spectral indices are related by

$$n_s - 1 = -\frac{3}{5} n_{\text{iso}} = -\frac{3}{8} n_g. \quad (87)$$

---

[1] A. H. Guth, Phys. Rev **D23**, 347 (1981).

- [2] A. Albrecht and P. J. Steinhardt, Phys. Rev. Lett. **48** (1982) 1220; A. Linde, Phys. Lett. **108B**, 389 (1982).
- [3] A. Linde, Phys. Lett. **129B**, 177 (1983).
- [4] E. Gliner and I. G. Dymnikova, Sov. Astron. Lett. **1**, 93 (1975); R. Brout, F. Englert and E. Gunzig, Ann. Phys. **115**, 78 (1978); A. A. Starobinsky, Phys. Lett. B **91**, 154 (1980); L. Z. Fang, Phys. Lett. B **95**, 154 (1980); E. Kolb and S. Wolfram, Astrophys. J. **239**, 428 (1980); K. Sato, Phys. Lett. B **99**, 66 (1981); D. Kazanas, Astrophys. J. **241**, L59 (1980); for a further review on the early development of inflationary cosmology please see K. A. Olive, Phys. Rep. **190**, 307 (1990).
- [5] A. Liddle, In proc. of ICTP summer school in high-energy physics, 1998 (astro-ph/9901124)
- [6] J. Yokoyama, A. Linde, Phys. Rev. **D60**, 083509 (1999).
- [7] L. Kofman, A. Linde, A. Starobinsky, Phys. Rev. **D56**, 3258 (1997).
- [8] B. A. Bassett, F. Tamburni, D. L. Kaiser and R. Maartens, Nucl. Phys. **B561**, 188 (1999); B.A. Bassett, C. Gordon, R. Maartens, D.I. Kaiser, Phys. Rev. **D61**, 061302 (2000).
- [9] F. Finelli and R. Brandenberger, Phys. Rev. Lett. **82**, 1362 (1999).
- [10] M. Parry and R. Easther, Phys. Rev. **D59**, 061301 (1999).
- [11] A. Liddle, D.H. Lyth, K.A. Malik, D. Wands (hep-ph/9912473)
- [12] A. Berera and L. Z. Fang, Phys. Rev. Lett. **74**, 1912 (1995).
- [13] A. Berera, Phys. Rev. Lett. **75**, 3218 (1995).
- [14] A. Berera, In Press, Nuclear Physics B, (2000) (hep-ph/9904409).
- [15] A. Berera, Phys. Rev. **D54**, 2519 (1996).
- [16] E. Gunzig, R. Maartens, and A. V. Nesteruk, Class. Quant. Grav. **15**, 923 (1998).
- [17] H. P. de Oliveria and R. O. Ramos, Phys. Rev. **D57**, 741 (1998).
- [18] M. Bellini, Phys. Lett. **B428**, 31 (1998).
- [19] J. M. F. Maia and J. A. S. Lima, Phys. Rev. **D60**, 101301 (1999).
- [20] A. Berera, Phys. Rev. **D55**, 3346 (1997)
- [21] A. Berera, M. Gleiser and R. O. Ramos, Phys. Rev. **D58**, 123508 (1998).
- [22] A. Berera, M. Gleiser and R. O. Ramos, Phys. Rev. Lett. **83**, 264 (1999).
- [23] A. Berera and T. W. Kephart, Phys. Lett. **B456**, 135 (1999).
- [24] A. Berera and T. W. Kephart, Phys. Rev. Lett. **83**, 1084 (1999).
- [25] A. R. Liddle and D. H. Lyth, Phys. Rept. **231**, 1 (1993).
- [26] D. Wands, K.A. Malik, D.H. Lyth, A.R. Liddle, 2000 (astro-ph/0003278)
- [27] B. J. Carr, J. H. Gilbert, and J. E. Lidsey, Phys. Rev. **D50**, 4853 (1994); E. Kotok and P. Naselsky, Phys. Rev. **D58**, 103517 (1998).
- [28] A. Berera, L. Z. Fang, and G. Hinshaw, Phys. Rev. **D57**, 2207 (1998).
- [29] W. Lee and L. Z. Fang, Int. J. Mod. Phys. **D6**, 305 (1997).
- [30] M. Tegmark, M. Zaldarriaga, ApJLett, in press 2000 (astro-ph/0002091).
- [31] U. Seljak, M. Zaldarriaga, ApJ **469**, 437 (1996).